



Microstructure of creep-deformed V–4Cr–4Ti strengthened by precipitation and cold rolling

T. Muroga^{a,*}, T. Nagasaka^a, J.M. Chen^b, Y.F. Li^c, H. Watanabe^d

^aNational Institute for Fusion Science, Oroshi, Toki, Gifu 509-5292, Japan

^bSouthwestern Institute of Physics, P.O. Box 432, Chengdu 610041, China

^cThe Graduate University for Advanced Studies, 322-6 Oroshi, Toki, Gifu 509-5292, Japan

^dResearch Institute for Applied Mechanics, Kyushu University, Kasuga, Fukuoka 816-8580, Japan

A B S T R A C T

The microstructural processes were investigated for V–4Cr–4Ti alloys strengthened by precipitation and cold rolling during thermal creep deformation and thermal aging in identical conditions at 1023 K. Cold rolling to precipitate-hardened V–4Cr–4Ti can suppress precipitate coarsening during the following high temperature aging. The dislocations observed were mixture of $a\langle 100 \rangle$ and $a/2\langle 111 \rangle$ types in the specimens with only thermal aging, and predominantly of $a/2\langle 111 \rangle$ type in the specimens after the creep deformation. Coarsening of the precipitates was observed after the creep deformation. It seems to be essential to avoid the recovery of sessile $a\langle 100 \rangle$ type dislocations induced by cold rolling for the purpose of maintaining the high temperature strength.

© 2008 Elsevier B.V. All rights reserved.

1. Introduction

One of the factors limiting the upper operation temperature of vanadium alloys is thermal creep performance [1–3]. Among the means to enhance the high temperature strength of the reference V–4Cr–4Ti alloys is to induce high density of precipitates in the matrix [4,5].

Recently, efforts were made by the authors to apply two-step heat treatments to V–4Cr–4Ti for the purpose of introducing high density of small Ti–CON precipitates followed by cold rolling [6]. The purpose of the cold rolling was to retard precipitate coarsening during high temperature aging. The treatment was shown to suppress steady creep deformation rate at high applied stress [6]. However, microstructural processes of the creep deformation remain to be investigated.

The objective of the present study is to obtain insight into the mechanism of the effect of thermal and mechanical treatment on the creep performance, with respect to the evolution of dislocations and precipitates.

2. Experimental

The material used in this study was the reference V–4Cr–4Ti alloy named NIFS-Heat-2 [3]. The as-received alloy plates were 0.5–1 mm thick and in the cold rolled state of >90% reduction in thickness. The specimens of 0.25 mm thick for the creep tests were cut

from these plates. Four thermal and mechanical treatments were applied to these plates, which are summarized in Table 1 [6]. All the heat treatments were performed in a high vacuum furnace better than 1×10^{-4} Pa. Samples were sandwiched with Ta plates and wrapped with Zr foil as a gaseous impurity getter. Specimens were cut or punched-out from 0.25 mm thick plates. The creep test specimens had the gauge dimension of $5 \times 1.2 \times 0.25$ mm³ (SS-J size).

Creep test was conducted for STD and SAACW specimens at 1023 K with the applied tensile stress of 176 and 250 MPa in vacuum of $<4 \times 10^{-5}$ Pa using a uniaxial creep testing machine for miniaturized tensile test specimens. Uniaxial and constant load was applied to the specimen by load blocks. A Zr foil surrounded the specimen during the test acting as an oxygen impurity getter. The creep tests started after the load and displacement signals recorded by the computer became stable, which took about 7 h, and finished at the strain level of 2.5–5%. For microstructure analysis by transmission electron microscope (TEM), 3 mm disks were punched-out from the gauge area of the specimens after the creep test. TEM observations were carried out using JEM-2000FX at RIAM, Kyushu University.

For comparison, thermal aging of SAA, STDCW, SAACW specimens was carried out in heat histories identical to those of the creep tests.

3. Results

Fig. 1 shows the creep strain as a function of the loading time. For both cases of the applied stress, SAACW specimens showed

* Corresponding author.

E-mail address: muroga@nifs.ac.jp (T. Muroga).

Table 1
The thermal and mechanical treatment conditions of the V–4Cr–4Ti (NIFS-Heat-2).

Abbreviation	Treatment	Conditions
STD	Standard	1273 K, 2 h
STDCW	Standard and Cold-rolled	STD + 20% Cold Rolled
SAA	Solution Annealed and Aged	1373 K, 1 h + 873 K, 20 h
SAACW	Solution Annealed, Aged and Cold-rolled	SAA + 20% Cold Rolled

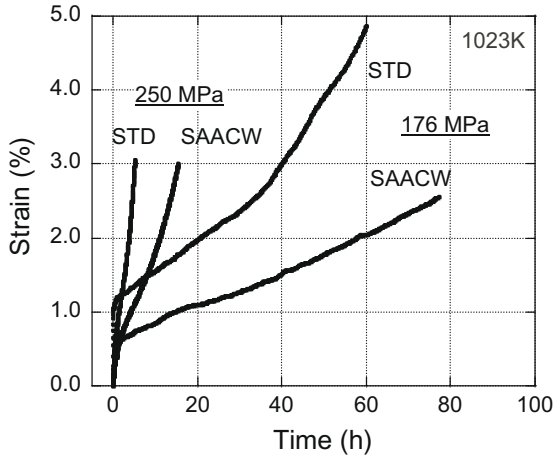


Fig. 1. Creep deformation behavior for STD and SAACW specimens at 1023 K.

lower creep strain rate than STD specimens. The tests were terminated at the end of the data lines for TEM observation.

Fig. 2 compares microstructure of SAACW after creep deformation for 80 h with 176 MPa at 1023 K and after the identical heat treatment (80 h at 1023 K) without any applied stress. In the case of after creep deformation, the direction of the applied tensile force is shown on the photograph. The photographs clearly show the difference in the dislocation morphology. After creep deformation, most dislocations are oriented to particular directions, while with only thermal aging, directions of the dislocations are more complex. Identification of the Burgers vector of the dislocation was carried out using a $\mathbf{g} \times \mathbf{b} = 0$ technique. The result showed that the dislocations were predominantly of $\mathbf{a}/2\langle 111 \rangle$ type in the specimen

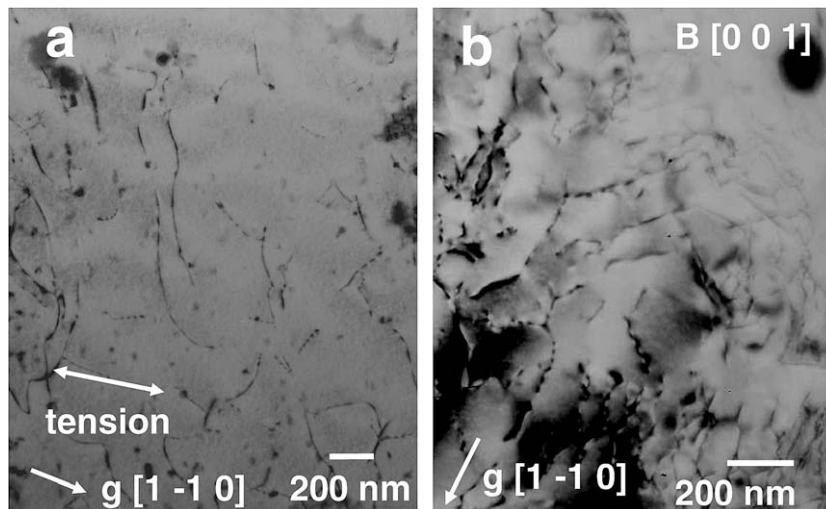


Fig. 2. Dislocation structure of SAACW specimens after (a) creep deformation with 176 MPa at 1023 K for 80 h, and (b) thermal aging in an identical thermal condition (1023 K, 80 h).

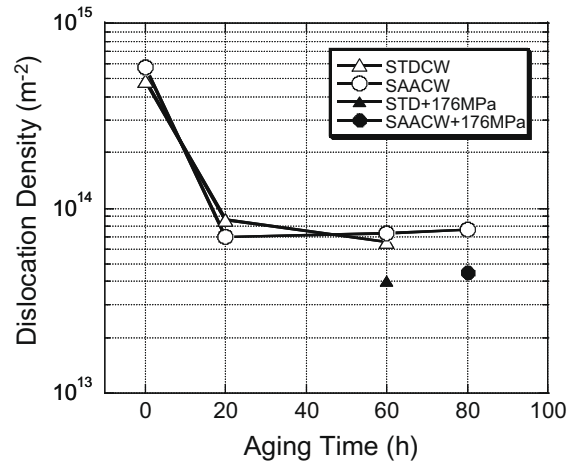


Fig. 3. Dislocation density as a function of the aging time at 1023 K for STDCW and SAACW. Dislocation densities of STD and SAACW specimens after creep tests with 176 MPa at 1023 K for 60 and 80 h, respectively, are also indicated.

after the creep deformation either with 176 or 250 MPa, and mixture of $\mathbf{a}\langle 100 \rangle$ and $\mathbf{a}/2\langle 111 \rangle$ types in the specimens with only thermal aging.

Fig. 3 shows dislocation density as a function of the aging time at 1023 K for STDCW and SAACW. Dislocation densities after the creep test with 176 MPa for 80 h at 1023 K are also shown. The figure shows that recovery of the dislocations induced by cold rolling was enhanced by the applied stress for SAACW. Also shown by comparison between STDCW and SAACW data is that the effects of SAA treatment on the recovery of the dislocations induced by cold rolling is small.

Fig. 4 compares microstructure of SAA, SAACW after aging at 1023 K for 80 h, and SAACW after creep deformation at 1023 K with 176 MPa for 80 h and with 250 MPa for 15 h. In these cases the micrographs were taken in off-Bragg imaging conditions showing exclusively the precipitate morphology. Precipitates were coarsened by the aging in SAA specimens. Because of high density of dislocations, precipitates did not grow in SAACW specimens by the aging. On the other hand, growth of precipitates was observed after the creep deformation of SAACW specimens. **Fig. 5** shows evolution of the precipitate size and density with the aging time at 1023 K

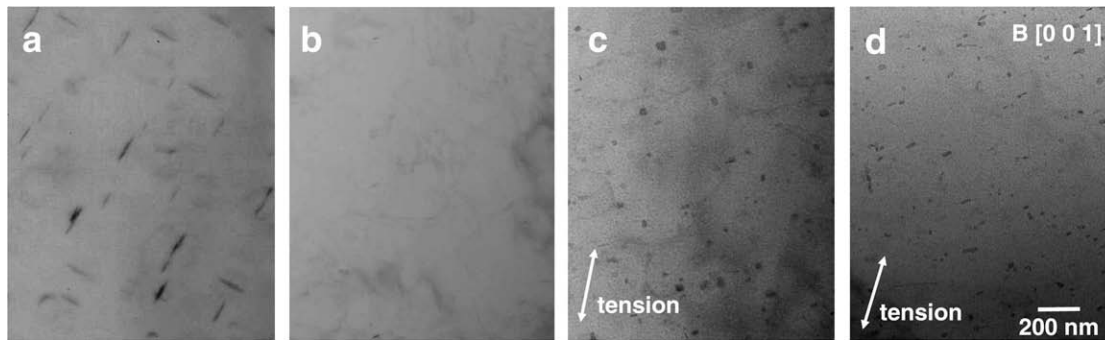


Fig. 4. Microstructure of (a) SAA and (b) SAACW specimens after aging at 1023 K for 80 h, and SAACW specimens after creep deformation at 1023 K with (c) 176 MPa for 80 h and with (d) 250 MPa for 15 h. The micrographs were taken in off-Bragg imaging conditions showing exclusively the precipitate images.

for SAA specimens. The precipitate size increased and the precipitate density decreased with the aging time for SAA specimens. Note that precipitate growth was not observed in SAACW specimens by the aging at 1023 K but observed after the creep tests. The data in ellipses are SAACW after the creep deformations. With the applied stress for creep deformation, however, the precipitate size is significantly smaller both for 176 and 250 MPa than those in SAA specimens after aging. The results show that a certain role to retard precipitate coarsening may remain in SAACW specimens after the recovery of the cold rolled dislocations.

4. Discussion

TEM examinations after creep deformation of V–4Cr–4Ti were reported for the specimens prepared from the pressurized creep tubes [7,8], in which dislocations observed were predominantly of $a/2\langle 111 \rangle$ type. This is consistent with the present study, which also showed the conversion of cold rolling induced dislocations composed of the mixture of $a/2\langle 111 \rangle$ and $a\langle 100 \rangle$ types to creep-induced dislocations of $a/2\langle 111 \rangle$ type.

It is known that in most BCC metals, $a\langle 100 \rangle$ type dislocations can be formed by interaction of $a/2\langle 111 \rangle$ type dislocations on different planes during the cold rolling process. Since $a\langle 100 \rangle$ type dislocations are sessile, they are thought to be stable and contribute to suppressing the precipitate coarsening and thus maintaining the high temperature strength. In contrast to cold rolling, creep

deformation by uniaxial loading is expected to induce only small chance for interaction of $a/2\langle 111 \rangle$ type dislocations with different planes forming $a\langle 100 \rangle$ type dislocations, because the deformation is expected to be induced by $a/2\langle 111 \rangle$ type dislocations on planes in limited directions. Therefore, recovery of cold rolling induced $a\langle 100 \rangle$ type sessile dislocations replacing with slippery $a/2\langle 111 \rangle$ type dislocations during the creep deformation is considered to be the reason for the precipitate growth.

It seems to be essential to prevent from the recovery of $a\langle 100 \rangle$ type dislocations for the purpose of maintaining the high temperature strength, including the creep resistance. For this purpose, the materials need to be used at the temperature range and load level where $a\langle 100 \rangle$ type dislocations should not recover. It will also be a direction for improvement to enhance the stability of the dislocations by metallurgical efforts such as minor element addition and so on.

The smaller precipitate size in SAACW specimens after creep deformation than that in SAA specimens after identical aging, shown in Fig. 5, suggests that the precipitate growth was suppressed during the creep deformation by the influence of gliding creep dislocations. Alternatively, the beginning of the precipitate growth could be delayed in the case of creep deformation of SAACW specimens because of the time necessary for recovering the cold rolling induced dislocations. However, the similar density but much smaller size of precipitates observed after the creep deformation implies that the creep deformation suppressed precipitate growth process than the nucleation and coalescence processes.

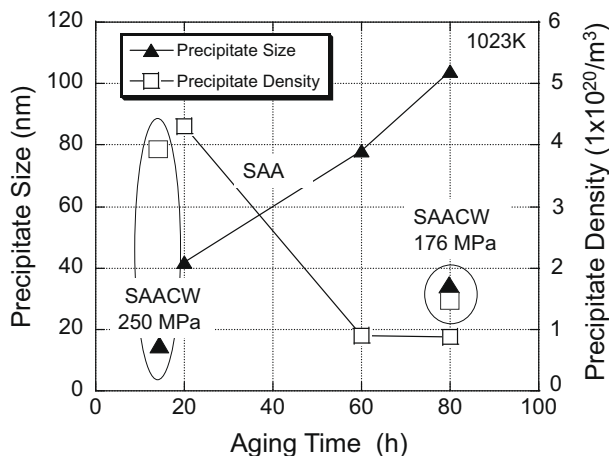


Fig. 5. The evolution of precipitate size and density with the aging time at 1023 K for SAA specimens. The data in ellipses are for SAACW specimens after the creep deformations. Note that precipitate growth was not observed in SAACW specimens by the aging at 1023 K.

5. Conclusion

The microstructural processes of the effects of precipitation and cold rolling of V–4Cr–4Ti on creep deformation performance were investigated. The cold rolling to the precipitate-hardened V–4Cr–4Ti can suppress the precipitate coarsening during high temperature aging. The dislocations were mixture of $a\langle 100 \rangle$ and $a/2\langle 111 \rangle$ types in the specimens with only thermal aging, and predominantly of $a/2\langle 111 \rangle$ type in the specimens after the creep deformation. The loss of cold rolling induced sessile $a\langle 100 \rangle$ type dislocations resulted in the coarsening of precipitates. It seems to be essential to prevent from the recovery of $a\langle 100 \rangle$ type dislocations for the purpose of maintaining the high temperature strength of precipitate-hardened V–4Cr–4Ti.

Acknowledgements

This work was carried out based on NIFS Budget Code NIFS07UCFF003. This work was also supported by JSPS-CAS Core University Program.

References

- [1] T. Muroga, J.M. Chen, V.M. Chernov, K. Fukumoto, D.T. Hoelzer, R.J. Kurtz, T. Nagasaka, B.A. Pint, M. Satou, A. Suzuki, H. Watanabe, *J. Nucl. Mater.* 367–370 (2007) 780.
- [2] R.J. Kurtz, K. Abe, V.M. Chernov, D.T. Hoelzer, H. Matsui, T. Muroga, G.R. Odette, *J. Nucl. Mater.* 329–333 (2004) 47.
- [3] T. Muroga, T. Nagasaka, K. Abe, V.M. Chernov, H. Matsui, D.L. Smith, Z.-Y. Xu, S.J. Zinkle, *J. Nucl. Mater.* 307–311 (2002) 547.
- [4] J.M. Chen, T. Muroga, T. Nagasaka, S.Y. Qiu, C. Li, Y. Chen, B. Liang, Z.Y. Xu, *Fusion Eng. Des.* 81 (2006) 2899.
- [5] T. Muroga, T. Nagasaka, A. Nishimura, J.M. Chen, *Mater. Sci. Forum* 475–479 (2005) 1449.
- [6] J.M. Chen, T. Nagasaka, T. Muroga, S.Y. Qiu, C. Li, N. Nita, *J. Nucl. Mater.* 374 (2008) 298.
- [7] D.S. Gelles, *J. Nucl. Mater.* 307–311 (2002) 393.
- [8] K. Fukumoto, S. Takahashi, R.J. Kurtz, D.L. Smith, H. Matsui, *J. Nucl. Mater.* 341 (2005) 83.